Individually-addressable flip-chip AlInGaN micropixelated light emitting diode arrays with high continuous and nanosecond output power

H. X. Zhang,[1] D. Massoubre,[1] J. McKendry,[1] Z. Gong,[1] B. Guilhabert,[1] C. Griffin,[1] E. Gu,[1,*] P.E. Jessop,[1,2] J. M. Girkin,[1] and M. D. Dawson[1]

[1] *Institute of Photonics, University of Strathclyde, Wolfson Centre, 106 Rottenrow, Glasgow G4 0NW, UK*
[2] *Permanent address: Dept of Engineering Physics, McMaster University, Hamilton, Ontario, Canada*
**Corresponding author: erdan.gu@strath.ac.uk*

Abstract: Micropixelated blue (470nm) and ultraviolet (370nm) AlInGaN light emitting diode ('micro-LED') arrays have been fabricated in flip-chip format with different pixel diameters (72μm and 30μm at, respectively, 100 and 278 pixels/mm^2). Each micro-LED pixel can be individually-addressed and the devices possess a specially designed n-common contact incorporated to ensure uniform current injection and consequently uniform light emission across the array. The flip-chip micro-LEDs show, per pixel, high continuous output intensity of up to 0.55μW/μm^2 (55W/cm^2) at an injection current density of 10kA/cm^2 and can sustain continuous injection current densities of up to 12kA/cm^2 before breakdown. We also demonstrate that nanosecond pulsed output operation of these devices with per pixel on-axis average peak intensity up to 2.9μW/μm^2 (corresponding to energy of 45pJ per 22ns optical pulse) can be achieved. We investigate the pertinent performance characteristics of these arrays for micro-projection applications, including the prospect of integrated optical pumping of organic semiconductor lasers.

OCIS codes: (230.3670) Light emitting diodes; (230.3990) Micro-optical devices, (220.4000) Microstructure fabrication, (230.6080) Sources, (180.1790) Confocal microscopy.

References and links

1. H. X. Jiang, S.X. Jin, J. Li, J. Shakya, and J.Y. Lin, "III-nitride blue microdisplay," Appl. Phys. Lett. **78**, 1303-1305 (2001).
2. I. Ozden, M. Diagne, A.V. Nurmikko, J. Han, and T. Takeuchi, "Matrix-addressable 1024 element blue light emitting InGaN QW diode array," Phys. Stat. Solidi (a) **188**, 139 (2001).
3. V. Adivarahan, S. Wu, W. H. Sun, V. Mandavilli, M. S. Shatalov, G. Simin, J. W. Yang, H. P. Maruska, and M. A. Khan, "High-power deep ultraviolet light-emitting diodes based on a micro-pixel design," Appl. Phys. Lett. **85**, 1838-1840 (2004).
4. C. W. Jeon, H. W. Choi, E. Gu, and M. D. Dawson, "High-density matrix-addressable AlInGaN-based 368nm microarray light-emitting diodes," IEEE Photon. Technol. Lett. **16** (11), 2421-2423 (2004).
5. H. W. Choi, C. W. Jeon, and M.D. Dawson, "High-resolution 128x96 nitride microdisplay," IEEE Electron Dev. Lett. **25** (5), 277-279 (2004).
6. H. X. Zhang, E. Gu, C. W. Jeon, Z. Gong, M. D. Dawson, M. A. A. Neil, and P. M. W. French, **"**Microstripe-array InGaN light-emitting diodes with individually addressable elements,**"** IEEE Photon. Technol. Lett. **18** (15), 1681-1683 (2006).
7. C. W. Jeon, E. Gu, and M.D. Dawson, "Mask-free photolithographic exposure using a matrix-addressable micropixellated AlInGaN ultraviolet light-emitting diode," Appl. Phys. Lett. **86**, 221105 (2005).
8. H. Peng, E. Makarona, Y. He, Y. K. Song, A. V. Nurmikko, J. Su, Z. Ren, M. Gherasimova, S.-R. Jeon, G. Cui, J. Han, "Ultraviolet light-emitting diodes operating in the 340nm wavelength range and application to time-resolved fluorescence spectroscopy," Appl. Phys. Lett. **85**, 1436 (2004).
9. V. Poher, H. X. Zhang, G. T. Kennedy, C. Griffin, S. Oddos, E. Gu, D. S. Elson, J.M. Girkin, P.M.W. French, M.D. Dawson and M.A.A. Neil**,** "Optical sectioning microscopes with no moving parts using a micro-stripe array light emitting diode," Opt. Express **15** (18), 11196-11206 (2007).

10. E. Gu, H. X. Zhang, H. D. Sun, M. D. Dawson, A. R. Mackintosh, A. J. C. Kuehne, R. A. Pethrick, C. Belton and D. D. C. Bradley, "Hybrid inorganic/organic microstructured light-emitting diodes produced using photocurable polymer blends," Appl. Phys. Lett. **90**, 031116 (2007).
11. B.R. Rae, C. Griffin, J. McKendry, J.M. Girkin, H.X. Zhang, E. Gu, D. Renshaw, E. Charbon, M.D. Dawson, and R.K. Henderson, "CMOS driven micro-pixel LEDs integrated with single photon avalanche diodes for time resolved fluorescence measurements," J. Phys. D: Applied Physics **41**, 094011 (2008).
12. J. A. Chediak, Z. Luo, J. Seo, N. Cheung, L. P. Lee, and T. D. Sands, "Heterogeneous integration of CdS filters with GaN LEDs for fluorescence detection microsystems," Sens. Actuators A. **111**, 1-7 (2004).
13. P. Y. Chiou, A. T. Ohta and M. C. Wu, Nature, "Massively parallel manipulation of single cells and microparticles using optical images," Nature **436**, 370-372, (2005).
14. C. Karnutsch, C. Pflumm, G. Heliotis, J. C. deMello, D. D. C. Bradley, J. Wang, T. Weimann, V. Haug, C. Gärtner, and U. Lemmer,, "Improved organic semiconductor lasers based on a mixed-order distributed feedback resonator design," Appl. Phys. Lett. **90**, 131104 (2007).
15. Z. Gong, H.X. Zhang, E. Gu, C. Griffin, M.D. Dawson, V. Poher, G. Kennedy, P.M.W. French, and M.A.A. Neil, "Matrix-addressable micropixellated InGaN light-emitting diodes with uniform emission and increased light output," IEEE Trans. Electron. Dev. **54**, 2650 (2007).
16. V. Adivarahan, Q. Fareed, S. Srivastaka, T. Katona, M. Gaevski and A. Khan, "Robust 285nm deep UV light emitting diodes over metal organic hybride vapor phase eptaxially grown AlN/Sapphire templates," Jpn J. Appl. Phys. **46** (23), L537-L539 (2007).
17. X. Guo and E. F. Schubert, "Current crowding and optical saturation effects in GaInN/GaN light emitting diodes grown on insulating substrates," Appl. Phys. Lett. **78**, 3337-3339 (2001).
18. Nils Hempler, John-Mark Hopkins, Alan J. Kemp, Nico Schulz, Marcel Rattunde, Joachim Wagner, Martin D. Dawson and David Burns**, "**Pulsed pumping of semiconductor disk lasers," Opt. Express **15 (**6), 3247-3256 (2007).
19. E. Gu, H. W. Choi, G. McConnell, A. M. Gurney, C. Liu, C. Griffin, J. M. Girkin, I. M. Watson and M. D. Dawson , "Reflection/transmission confocal microscopy characterization of single-crystal diamond microlens arrays," Appl. Phys. Lett. **84**, 2754-2756 (2004).
20. C. Griffin, E. Gu, H. W. Choi, C. W. Jeon, J. M. Girkin and M. D. Dawson, "Beam divergence measurements of InGaN/GaN micro-array light emitting diodes using confocal microscopy," Appl Phys. Lett. **86**, 041111 (2005).
21. J.M. Girkin, D. L. Wokosin, A. M. Gurney and A. I. Ferguson, "Confocal microscopy using InGaN violet laser diode at 406nm," Opt. Express **7** (10), 336-341 (2000).
22. I. Moreno and C.-C. Sun, "Modeling the radiation pattern of LEDs," Opt. Express **16** (3), 1808-1819 (2008).
23. K. Kawasaki, C. Koike, Y. Aoyagi and M. Takeuchi, "Vertical AlGaN deep ultraviolet light emitting diode emitting at 322nm fabricated by the laser lift-off technique," Appl Phys. Lett. **89**, 261114 (2006).

1. Introduction

Gallium nitride micro-sized light-emitting diode ('micro-LED') arrays at visible and ultraviolet (UV) wavelengths have been the subject of growing interest over recent years [1-6]. These versatile micro-structured sources can be pattern-programmed under computer control to project fixed or high frame rate optical images, for spatially and spectrally selective excitation of a wide range of materials. This capability is opening up instrumentation and scientific applications in areas as diverse as mask-free photolithography and direct writing, optical sectioning microscopy, hybrid organic/inorganic devices, time-resolved fluorescence spectroscopy, and optical lab-on-a-chip [7-12].

Several of these applications require projected continuous intensities *per pixel* of >10nW/μm^2 [13]. A further exciting prospective use, in the integrated optical pumping of organic semiconductor lasers, requires nanosecond output of at least a few tens of pJ energy per pulse [14]. This raises the question of the best format of such a pixelated device to push the performance to the levels required by these more demanding applications and of how best to integrate them with control electronics. Most of the devices reported to date use an "epitaxy-up" configuration, where the light is extracted through the p-metal contact at the epitaxial surface. Although now successfully demonstrated in scalable and uniform matrix-addressable arrays [15], these devices generally compromise performance by optical losses in the p-contact, accentuated as the wavelength gets shorter, and electrical issues concerning the long conduction paths through the n-GaN or associated metal tracks. Because of these issues,

interest is developing in the flip-chip format of micro-LED devices, where the structure is inverted and light extracted though the (polished) sapphire epitaxial substrate. Adivarahan *et al.* [16], for example, who concentrated on continuous device performance in the deep ultraviolet, fabricated 285nm-wavelength flip-chip micro-LED's with 50µm-diameter emitting pixels showing no apparent power roll-over for a driving current density up to 3.5kA/cm^2. These pixels showed maximum output intensity as high as 300nW/µm^2. It was proposed that this intensity enhancement is mainly due to a more efficient current injection leading to better internal quantum efficiency and to improved thermal management [3].

Here we report advances in flip-chip micro-LED arrays where the elements are individually addressable in a format suitable for control via a complementary metal oxide silicon (CMOS) backplane. We concentrate on wavelengths of 370nm and 470nm, respectively, where a direct comparison can be made to earlier devices underpinning a range of applications demonstrators. Continuous output intensities (I_{out}) per pixel of up to 0.55µW/µm^2 were achieved at an injection current density of 10kA/cm^2. We show that these flip-chip pixels can sustain, in continuous operation, high injection current densities ~12kA/cm^2 before breakdown. In addition, we demonstrate two further important and defining characteristics of these devices. First, we investigated the nanosecond pulsed performance of these devices, showing that, per pixel, an on-axis beam peak intensity of 2.9µW/µm^2 at 200kA/cm^2 can be achieved before power saturation. This corresponds to energy of 45pJ per 22ns optical pulse, sufficient in principle to pump organic semiconductor lasers. Secondly, given the general applications focus on micro-projection and the facility for further integration offered by the sapphire upper window, we use confocal microscopy to characterize the intensity and spot size of the optical beam at the sapphire-to-air interface. We show that a trade-off between the pixel size and the sapphire substrate thickness is necessary to optimize the effective intensity available at the sapphire surface. Taken together, these results represent significant advances in micro-LED's suitable for a wide range of micro-systems applications.

2. Device fabrication

The flip-chip micro-LED devices each consist of an array of either 16 x 16 pixels (device type A, 100 pixels/mm^2) or 32 x 32 pixels (device type B, 278 pixel/mm^2). The former devices have a pixel diameter (D) of 72µm on a 100µm pitch and the latter have a pixel diameter of 30µm on a 60µm pitch. The epitaxial structures for 370nm and 470nm LED wafers, together with the overall device fabrication sequence, are similar to those reported earlier for the 'epi-up' devices [4, 5]. The mesa structure of each individual micro-LED was first defined by standard photolithographic patterning and inductively coupled plasma (ICP) etching. Then, a pre-metallization HCl acid treatment was applied and thick Ni/Au spreading contacts were evaporated on the *p*-contact area, to act as a combined contact/mirror. The contacts were alloyed by rapid thermal annealing (RTA) in air. The *n*-type metallization was formed by Ti/Au deposition to fill the area between each of the LED elements. Even though one pad would in principle be sufficient to connect the shared *n*-common contact, here we used four *n*-pads, one on each side of the array (Fig. 1(a)), to improve the uniformity of the current spreading. Finally, a SiO_2 protective layer was deposited and patterned by plasma enhanced chemical vapour deposition and reactive ion etching. To facilitate the further device integration, the sapphire substrate of each device was thinned down to 80µm and polished. The devices were specifically designed for flip-chip bonding to a silicon/CMOS backplane, as reported elsewhere [11]. However, to facilitate the tests reported here, the micro-LED arrays were bonded onto printed circuit boards. All the measurements were performed using the through-sapphire (back side) emission.

3. Characterization in continuous and pulsed modes

Fig. 1(a) shows a microphotograph of a portion of a 16 x 16 flip-chip micropixelated LED array (type A) with the image taken through the polished sapphire substrate. A single (type A) and two (type B) blue operating pixels are shown on the images of Fig. 1(b) and (c), respectively. A single and two UV operating pixels (type A) are also shown in the images of

Fig. 2(a) and (b). All these pictures are from representative devices. From these images, it can be seen that the light emission is uniform, not only within each pixel, but also from pixel to pixel. We note that the pixel sidewalls are angled, to reflect light upwards; light reflected at the pixel sidewalls is evident in the Figs.

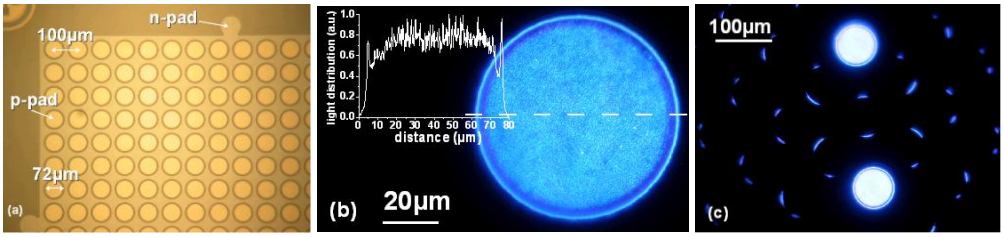

Fig. 1. (a) Microscope image of a typical type A device taken through the polished sapphire substrate and showing a portion of the 16 x 16 micro-pixel array with two *n*-pads (on the left and top sides of the image), (b) a representative single operating blue pixel from a type A device with in inset the light distribution along the dashed line, and (c) light emitted by two close pixels from a type A device.

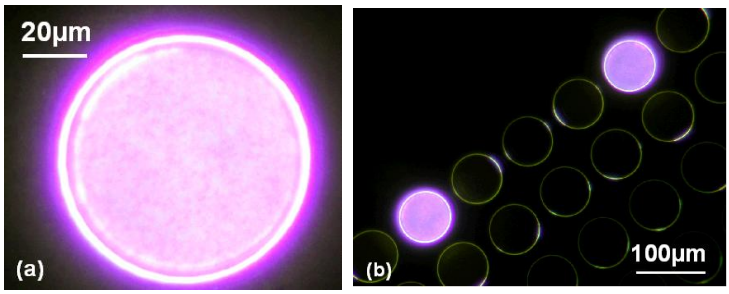

Fig. 2. Microscope images taken through the sapphire substrate of, respectively, (a) a representative single operating UV pixel and (b) representative pair of UV pixels. Both images are from a type A device.

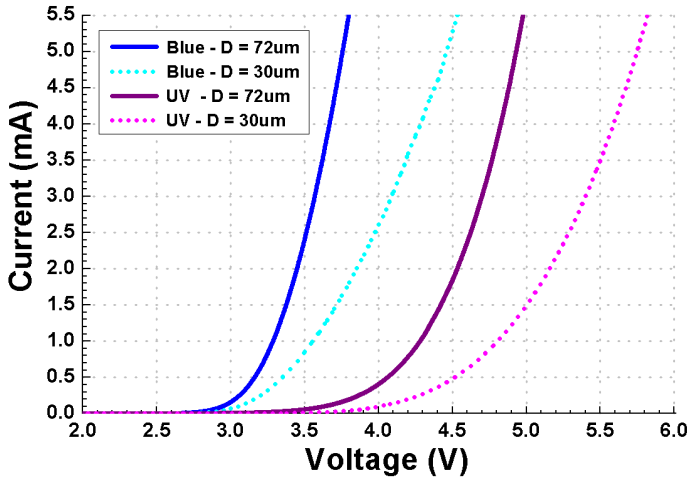

Fig. 3. Single pixel I - V characteristics of blue and UV flip-chip micro-LED type A and B devices.

Fig. 3 shows typical current vs. voltage (I-V) characteristics of representative single LED pixels from the different arrays, performed under direct current (DC) bias conditions at room

temperature. Each entire flip-chip micro-pixelated LED array showed good electrical uniformity; measurements made on several randomly selected pixels on samples of both types of device at the two wavelengths have shown a low variation for both the turn-on voltage (V_{on}) and the series resistance (R_s) of, respectively, 0.1V and 5Ω. We attribute this good uniformity to the specially designed Ti/Au *n*-contact, which fills the area between the LED elements and facilitates uniform current spreading. The typical values per pixel for V_{on} and R_s are reported in Table 1. As expected, the higher energy bandgap of the UV material and its poorer crystalline quality led to a higher turn-on voltage than for the blue wavelength devices. The series resistance is also increased when the pixel size is decreased due to the smaller surface area which increases the contact resistance [3].

Table 1. Typical electrical and optical characteristics per pixel for type A and type B devices at 470nm and 370nm.

	Type A (D = 72μm)		Type B (D = 30μm)	
	Blue (470nm)	UV (370nm)	Blue (470nm)	UV (370nm)
Turn–on Voltage (V)	3.2	4.3	3.4	4.8
Series Resistance (Ω)	110	130	220	190
Maximum output power per pixel (μW)	770@60mA	80@26mA	390@70mA	20@15mA
Maximum energy per pulse (pJ) at 10.5kHz, and corresponding optical pulse width	72@1.8A, 28ns	12@0.6A, 22ns	45@1.4A, 22ns	4@0.5A, 18ns

The experimental data from the continuous optical output power measurements of individual pixels are plotted in Fig. 4 and the maximum continuous output power per pixel for each device is summarized in Table 1. We note here that these measurements were taken with a calibrated optical power meter collecting light *exiting* the sapphire, with this power then normalized to the device active area. The current was also normalized to the active area, and the results – which allow direct comparison between the devices of different active areas - are shown in Fig.4. Two main results can be deduced from this data. Firstly, at a given pixel size and for the same injection current density, the blue emission devices present an output intensity much higher than the UV ones, which is expected mainly due to the poorer internal quantum efficiency of the UV active structure. Secondly, whatever the emission wavelength and despite their slightly higher turn-on voltages, the micro-LEDs with reduced size are able to sustain a much higher injection current density before roll-over (power saturation) appears. Indeed, whereas the blue (UV) type A device output power starts to decrease from a current density of 1.5kA/cm^2 (0.7kA/cm^2), the blue (UV) type B devices output power increases monotonically with current density up to 10kA/cm^2 (2kA/cm^2). The type B devices reach a maximum output optical intensity of 0.55μW/μm^2 and 0.029μW/μm^2, respectively, at wavelengths of 470nm and 370nm. For comparison, a conventionally processed top-emission LED, operating at 470nm with an emission area of 165μm by 305μm was also made. A maximum output intensity of 0.06μW/μm^2 was obtained for this device, indicating that a

micro-pixel of 30µm diameter fabricated by the new process provides an enhancement factor of 9 for the output intensity. Although not intended as a competitive format to broad area devices, we note here the performance comparison of our micro-pixel device to the broad area LED, when scaled with area and all micro-pixels on. The 'fill factor' of a 32x32 array is approximately 20% (that is, a fifth of the total area emits light). Taking this into account the effective output intensity is 0.11µW/µm^2 for the entire chip. Thus, with all pixels turned on, the device with a same entire area as the broad area LED would give a usable output power of 5535µW, compared to 3020µW for the broad area device, an increase of almost a factor of two. It should be emphasized that the type B micro-pixel device has the capability to endure extremely high current densities up to 12kA/cm^2 (blue) and 5.6kA/cm^2 (UV) before breakdown, which we believe to be the highest such results reported for nitride-based LEDs. One may expect even higher optical intensities if an optimized heat sink was employed. The improved optical performance of the device type B is likely to be due to the combined effect of higher light extraction efficiency, due to a higher wall surface to volume ratio, and reduced current crowding [17].

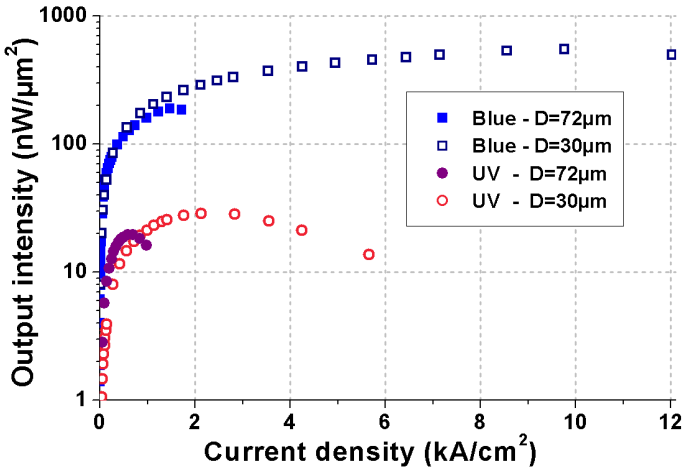

Fig. 4. Typical intensities versus injection current densities for blue and UV flip-chip micro-LEDs in type A and B device formats (densities calculated from the pixel area).

A promising application for such flip-chip micro-LED arrays is for optical pumping of integrated organic semiconductor lasers (OSL's). Given that objective, we also investigated type A & B devices under pulsed operation with the idea of obtaining nanosecond pulses with high energy per pulse. For this purpose, a custom laser diode driver providing high current pulses at low repetition rates was used [18]. With OSL pumping in mind, the repetition rate was tuned to 10.5kHz, which is a typical value used for that application [14] and the electrical pulse width was fixed at 18ns (driver limited), giving an optical pulse width in the same order of magnitude (from 18 to 28ns, dependent on the device type and injection current). The maximum energy per pulse obtained under these driving conditions is also reported in table 1 for each device. We note that higher energy pulses could readily be obtained by increasing the electrical pulse width: we have measured pulse energies of above 150pJ in 34ns optical pulses. Fig. 5 shows the main results obtained per pixel for devices A and B at 470nm and 370nm. To compare the results for the different pixel sizes, the measured (external to the sapphire) energy per pulse has been divided by the pixel area and by the pulse width at half maximum to provide an average peak intensity. The trends are similar to those observed in continuous mode, i.e. that the maximum average peak intensity (I_{peak}) is obtained with the smallest blue pixel size (device B). Nevertheless, for each device the intensity in the pulsed regime is much higher than the one measured in continuous mode due to the use of a low duty

cycle (~0.02%). Thus, an I_{peak} up to 2.9µW/µm^2 (corresponding to a density of energy of 6.4µJ/cm^2) was obtained for the blue device B (5-fold higher than in continuous mode) and up to 330nW/µm^2 (corresponding to a density of energy of 570nJ/cm^2) for the UV device B (11-fold higher than in continuous mode). We would also like to emphasize that the type B device has shown the capability to endure extremely high pulsed current densities up to 200kA/cm^2 (blue) and 72kA/cm^2 (UV) before breakdown. Such pulses are powerful enough to be used for 'indirect electrical' pumping of an OSL [14].

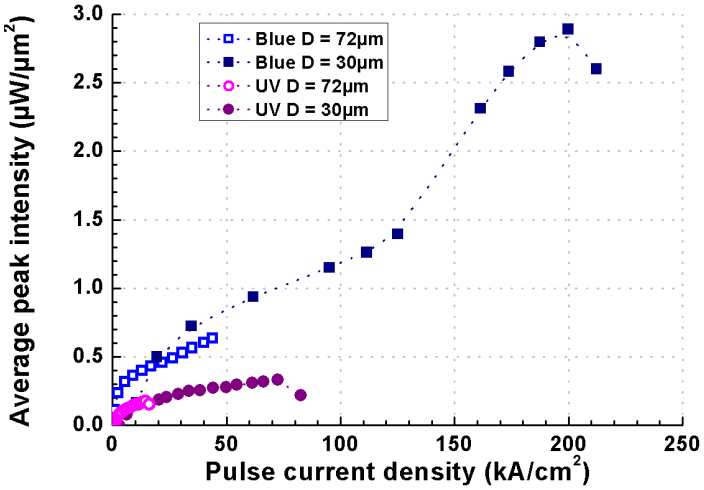

Fig. 5. Typical peak intensities versus pulsed current density characteristics per pixel for both types of devices at both wavelengths. The repetition rate was fixed at 10.5kHz with an electrical pulse width of 18ns.

4. Output beam characterization

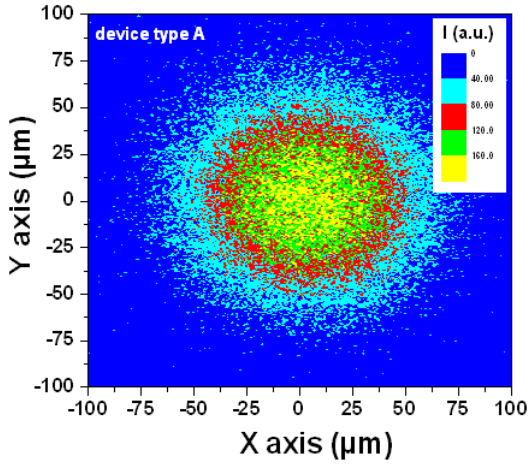

Fig. 6. Characteristic X-Y optical section (false color image) of a single pixel micro-LED output beam taken in air at the sapphire substrate surface for a blue type A device using confocal microscopy.

The flat and inert sapphire surface is well suited for micro-element integration such as OSL's or micro-fluidic channels. Due to the beam divergence within the sapphire substrate, the intensity (I_2) at this surface is lower than that at the micro-LED exit surface (I_1). Thus the effective intensity I_2 available for integrated opto-microfluidic applications is in fact lower than the intensity I_1 emitted by each micro-pixel. To investigate this effect, a commercial upright confocal microscope was used to measure the intensity distribution of individual micro-LED pixels *in air* at the sapphire surface [19, 20]. The scan head was coupled to an inverted microscope (Zeiss Axiovert 100) through the side port, and an objective lens (X20, 0.75NA) with a full collection angle larger than the LED beam divergence in air [20] was used to collect the micro-LED emission which was finally detected by a photomultiplier. Computer control of the microscope enabled complete *X-Y* optical sections through the LED beam to be obtained. In previous calibrations of this confocal system, the lateral resolution had been measured to be 0.25µm at a wavelength of 488nm [21]. From the light distribution of each optical section, the beam divergence from the micro-LED can be obtained. Fig. 6 shows a representative example of an *X-Y* optical section taken at the sapphire surface of a pixel from blue type A device taken using the confocal microscope. In order to improve the signal-to-noise ratio of the measured light distribution, and knowing that the LED radiation pattern is rotationally symmetric around the axis of propagation, the Cartesian coordinates of each data point were converted into polar coordinates and averaged as a function of the radial distance from the beam center.

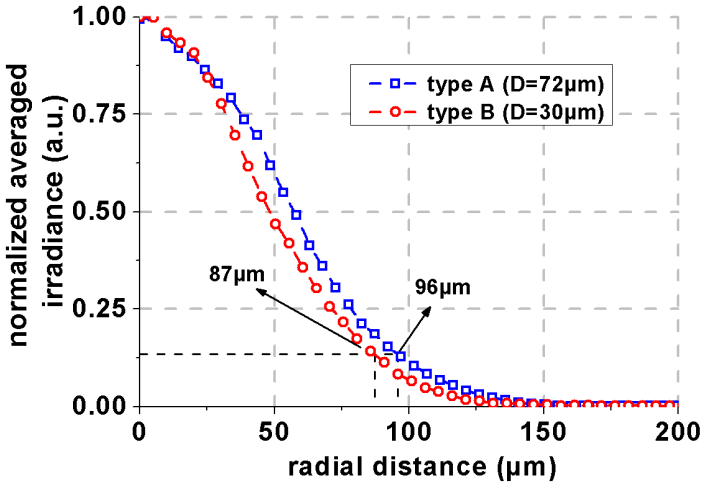

Fig. 7. Normalized irradiance versus the radial distance from the beam center for blue type A and B devices. The intensity was averaged around the beam center. The beam radii at $1/e^2$ of the maximum intensity are also indicated.

Fig 7 shows the normalized averaged irradiance versus the radial distance from the beam centre for both types of device. As expected, the spot size at the sapphire surface from the largest pixel shows a spot radius (determined at $1/e^2$ of the maximum intensity) larger than the one from the type B device which has a smaller pixel size, respectively 96µm versus 87µm. Nevertheless, the spot radius ratio presents a value smaller than the pixel diameter ratio, 1.1 instead of 2.4, which indicates that the output beam spreads out more rapidly within the sapphire substrate when the pixel size is reduced. This may be explained by the strong dependence of the beam divergence with the distance of propagation in the near field region, as the sapphire substrate thickness is smaller than the conventional limit between near field and far field conditions (five times the pixel size) [22]. By taking into account the spot sizes determined at $1/e^2$, we may calculate the maximum average effective intensity $I_{2\text{-max}}$ available at the sapphire surface for integrated applications and we obtain ratios $I_{2\text{-max}}/I_{1\text{-max}}$ of 0.14 and

0.03 with the type A and B devices respectively (no wavelength dependence being noticed on the beam divergence). These results show that while the intensity I_1 emitted by the micro-LEDs increases with decreasing pixel size, the intensity I_2 available at the surface of the 80µm-thick sapphire substrate drops more rapidly than would be expected with the smaller pixel size due to the beam divergence. As only the intensity at the sapphire surface matters for integrated applications, this means that in order to optimize I_2 there is a trade-off between the sapphire thickness and the pixel size. According to our experimental results, the intensity at the sapphire surface is maximal when the pixel size and the substrate thickness are similar. A solution to increase the effective intensity would thus be to further reduce the sapphire thickness allowing a decrease in the pixel size, though with a trade-off in mechanical handling/robustness. The optimum would be to completely remove the sapphire substrate, for instance by laser lift-off [23], in order to use the GaN surface as the surface (possibly planarized by a polymer film [7]) for micro-element integration.

5. Conclusion

In summary, micropixelated flip-chip AlInGaN light emitting diode arrays with varying pixel diameters, and designed for individual pixel addressing from a Si/CMOS backplane, have been fabricated at blue and UV wavelengths. Experimental results show that the pixel size reduction and the use of a large, shared n-contact enable a more uniform current injection at both a single pixel scale and at the array scale and consequently a more uniform light emission from the device. This current injection improvement combined with both the light extraction enhancement and the improved thermal management brought by the flip-chip configuration enable the micro-LEDs to produce higher continuous and pulsed output intensities and to withstand very high injection current densities. State of the art intensities per pixel up to 0.55µW/µm^2 in continuous mode and up to 2.9µW/µm^2 in pulsed mode were thereby obtained with a 30µm-size blue micro-LED array. Current densities up to 15kA/cm^2 in continuous (200kA/cm^2 in pulsed) mode were withstood before LED breakdown. Finally, confocal microscopy was also used to determinate the effective intensity available at the sapphire/air surface for future integration applications. The results show that a trade-off between the pixel size and the sapphire substrate thickness is necessary to optimise the effective intensity available at the sapphire surface because of the strong pixel size dependence of the beam divergence within the thin substrate. A good compromise is obtained for a pixel size similar to the sapphire thickness, the optimal solution being to totally remove the substrate. These results demonstrate that individually addressable flip-chip micro-LED arrays are promising candidates for applications including integrated organic semiconductor laser pumping and opto-microfluidics.

ACKNOWLEDGEMENT

This research work was supported by the UK Basic Technology Research Programme “A Thousand Micro-Emitters Per Square Millimetre: New Light on Organic Material & Structures”, by a Science and Innovation Award on “Molecular Nanometrology” and by the Scottish Consortium on Integrated Micro-photonic Systems.